The EMBO Journal vol.12 no.5 pp.1755-1765, 1993

Evidence for the involvement of PSI-E subunit in the reduction of ferredoxin by photosystem I

Françoise Rousseau, Pierre Sétif and Bernard Lagoutte

Section de Bioénergétique (CNRS, URA 1290), Département de Biologie Cellulaire et Moléculaire, Bâtiment 532, C.E.Saclay, 91 191, Gif-sur-Yvette, CEDEX, France

Communicated by J.-D.Rochaix

Of the stroma-accessible proteins of photosystem I (PSI) from *Synechocystis* sp. PCC 6803, the PSI-C, PSI-D and PSI-E subunits have already been characterized, and the corresponding genes isolated. PCR amplification and cassette mutagenesis were used in this work to delete the *psaE* gene. PSI particles were isolated from this mutant, which lacks subunit PSI-E, and the direct photoreduction of ferredoxin was investigated by flash absorption spectroscopy. The second order rate constant for reduction of ferredoxin by wild type PSI was estimated to be $\sim 10^9$ $M^{-1}s^{-1}$. Relative to the wild type, PSI lacking PSI-E exhibited a rate of ferredoxin reduction decreased by a factor of at least 25. After reassociation of the purified PSI-E polypeptide, the original rate of electron transfer was recovered. When a similar reconstitution was performed with a PSI-E polypeptide from spinach, an intermediate rate of reduction was observed. Membrane labeling of the native PSI with fluorescein isothiocyanate allowed the isolation of a fluorescent PSI-E subunit. Peptide analysis showed that some residues following the N-terminal sequence were labeled and thus probably accessible to the stroma, whereas both N- and C-terminal ends were probably buried in the photosystem I complex. Site-directed mutagenesis based on these observations confirmed that important changes in either of the two terminal sequences of the polypeptide impaired its correct integration in PSI, leading to phenotypes identical to the deleted mutant. Less drastic modifications in the predicted stroma exposed sequences did not impair PSI-E integration, and the ferredoxin photoreduction was not significantly affected. All these results lead us to propose a structural role for PSI-E in the correct organization of the site involved in ferredoxin photoreduction.

Key words: 2Fe-2S ferredoxin/cyanobacteria/flash-absorption spectroscopy/labeling/mutagenesis

Introduction

Photosystem I (PSI) is a supra-molecular complex located within the thylakoid membrane, catalyzing one of the two photochemical reactions in oxygenic photosynthesis. As a global result of complex electron transfer reactions, ferredoxin is reduced on the stromal face of the system and plastocyanin is oxidized on the lumenal face (reviewed in Golbeck and Bryant, 1991). The overall process appears to be quite similar in plants and cyanobacteria, the latter providing many advantages for genetic engineering. Since the first report on *Anacystis nidulans* (Shestakov and Khyen, 1970), several species of cyanobacteria have been shown to have a natural transformation system for the uptake of exogenous DNA (Porter, 1988; Haselkorn, 1991). When appropriate, this exogenous DNA can then be integrated in the genome by homologous recombination. In addition, some strains are capable of light-activated heterotrophic or chemoheterotrophic growth using a carbon source, thus allowing isolation of mutants severely impaired or even defective in photosynthesis (Vermaas *et al.*, 1986; Pakrasi *et al.*, 1988; Williams, 1988; Chauvat *et al.*, 1989; Anderson and McIntosh, 1991). Different genetic manipulations on central genes of PSI (*psaA*, *psaB* and *psaC*) recently illustrated these interesting possibilities (Mannan *et al.*, 1991; Smart *et al.*, 1991; Toelge *et al.*, 1991).

The PSI core complex has now been reported to comprise at least 12 proteins and the related genes have been cloned and sequenced. Most of these polypeptides are common to plants and cyanobacteria (Golbeck, 1992). Of the subunits exposed to the stromal face, PSI-D has been the subject of intense investigation. Several cross-linking experiments have shown its close association with PSI-C and PSI-E and its probable role in the docking of ferredoxin (Zanetti and Merati, 1987; Zilber and Malkin, 1988; Oh-Oka *et al.*, 1989). Reconstitution experiments demonstrated a function of this polypeptide in stabilizing the iron-sulfur centers Fe-S_A and Fe-S_B of PSI-C (Li *et al.*, 1991a). Inactivation of the *psaD* gene in *Synechocystis* 6803 resulted in a considerable decrease of P700 activity and a loss of integration of PSI-E, giving indirect evidence for the central role of PSI-D in the normal electron flow to soluble ferredoxin (Chitnis *et al.*, 1989a). Comparatively little is known concerning PSI-E, except its good accessibility to the stroma (Lagoutte and Vallon, 1992; Zilber and Malkin, 1992), and its close location to PSI-D, PSI-C (Oh-Oka *et al.*, 1989) and ferredoxin:$NADP^+$ oxidoreductase (EC 1.18.1.2) (FNR) (Andersen *et al.*, 1992). It has been reported that the inactivation of the corresponding gene in *Synechocystis* 6803 did not induce a significant decrease in PSI activity (Chitnis *et al.*, 1989b). This last result questions the exact function of this polypeptide, which is always found in PSI core complexes and is highly conserved.

We describe here some direct measurements of ferredoxin reduction using flash absorption spectroscopy, which gives direct access to the kinetics of electron flow to ferredoxin. PSI from various mutants of the PSI-E subunit, including a fully deleted mutant, have been analyzed by this functional approach and by classical biochemical techniques.

Results

Genetic constructions

The DNA fragment of 1529 bp obtained after PCR amplification, which contains the *psaE* gene, was cloned in

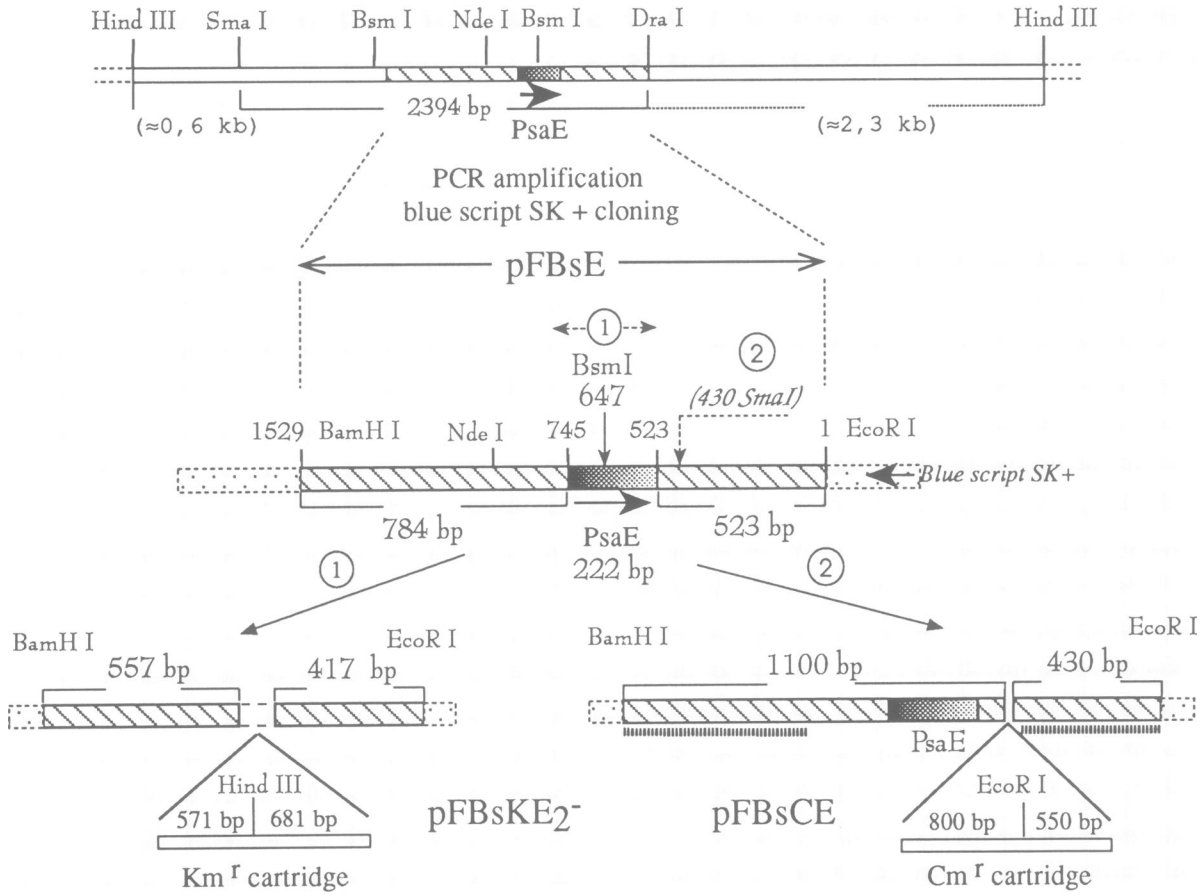

Fig. 1. Genetic constructions of the two plasmids for *psaE* deletion and *psaE* site-directed mutagenesis. A *Synechocystis* 6803 genomic fragment of 1529 bp containing *psaE* was amplified by the PCR technique with the creation of two flanking restriction sites (*Bam*HI and *Eco*RI). This PCR product was first inserted at the corresponding sites of a Bluescript SK^+ plasmid (Stratagene) to give the pFBsE plasmid. This plasmid was further engineered in two ways: (1) $pFBsKE_2^-$ was obtained after Bal31 digestion of *psaE* at the central *Bsm*I site; a Km^r cassette was then introduced at the place of the original *psaE* gene. (2) pFBsCE was generated by creating a unique *Sma*I site 93 bp downstream of *psaE*, opening the plasmid at this new restriction site, and inserting a Cm^r cassette. Dashed underlines are for the cyanobacterial sequences common to the two plasmids.

a Bluescript SK^+ plasmid using the *Eco*RI and *Bam*HI sites of the polylinker (Figure 1). We completely sequenced the cloned fragment using the two PCR primers and two others located on opposite strands, close to the middle of the *psaE* gene. In our strain, an AGA codon is found 28 bases after the starting ATG in place of the previously reported AGC (Chitnis *et al.*, 1989b). This finding confirms the difference at amino acid 9 previously observed in the protein sequence (Rousseau and Lagoutte, 1990), with the important consequence of an extra arginine in the N-terminal sequence of the protein instead of a serine. This construction in the Bluescript plasmid was named pFBsE. A first modification of this plasmid was designed to delete the *psaE* gene completely [Figure 1 (1)]. Cleavage of the plasmid was performed at the unique *Bsm*I site located close to the middle of the coding sequence. Bal31 exonuclease was then used to digest the plasmid symmetrically. The library of deleted plasmids was blunt-ended and ligated to the kanamycin resistance (Km^r) cassette from transposon Tn *903* (Pharmacia). A first selection was based on the expected resulting size of the plasmid DNA. The plasmid $pFBsKE_2^-$ was selected in this way, and the insertion sites of the Km^r cassette were fully sequenced. Deletion in this case extended 237 bp upstream of the original start codon and 106 bp downstream of the coding sequence. These deletions do not affect other open reading frames. The lengths of the remaining flanking sequences from the cyanobacterium are of 557 and 417 bp, still enough for homologous recombination after transformation. A second modification of the pFBsE plasmid was designed for reintroducing the *psaE* gene after site-directed mutagenesis [Figure 1 (2)]. A unique *Sma*I site was created 93 bp downstream of the coding sequence by an A to C change. After cleavage of the plasmid at this new site, a chloramphenicol resistance (Cm^r) cassette was introduced, thus leaving the full *psaE* coding sequence unaffected. This second plasmid was named pFBsCE; the only parts of cyanobacterial DNA homologous to the first deletion plasmid are the two outermost flanking sequences (dashed underlines). This latter construction allowed very efficient chloramphenicol selection for the reinsertion of mutated *psaE* copies as a recombination event inside the *psaE*/*cam*^{r} tandem is no longer possible in a *psaE*-deleted strain. This second plasmid was used for all site-directed mutagenesis experiments using a recipient strain firstly deleted for *psaE* using the first plasmid, $pFBsKE_2^-$.

Characterization of the psaE-deleted mutant

Molecular biology. A *Synechocystis* strain deleted for the *psaE* gene, named FKE_2, was obtained by transformation with the plasmid $pFBsKE_2^-$. The growth rate of the deleted strain, as followed by optical density measurements at 730 nm, was not less than the wild type when using the normal culture medium and a light intensity of 9 W/m^2. Southern analysis was used to check if all the original genomes were

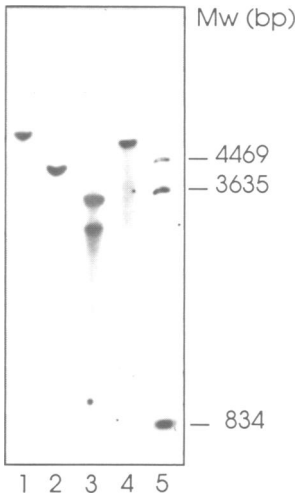

Fig. 2. Southern blot of genomic DNA from wild type and FKE_2 strains of *Synechocystis* 6803. Genomic DNA (2 μg) from the wild type (lanes 1 and 2) and the *psaE*-deleted strain FKE_2 (lanes 3 and 4), were digested by *Hin*dIII (lanes 1 and 3) or *Hin*cII (lanes 2 and 4) restriction enzymes and electrophoresed on a 0.8% agarose gel. Probing after transfer on a Hybond-N membrane was made with a digoxigenin-labeled fragment encompassing the *psaE* gene. Molecular weight markers (lane 5) were a mixture of *Bam*HI and *Ava*I fragments from the plasmid pFBsE detected with the same probe.

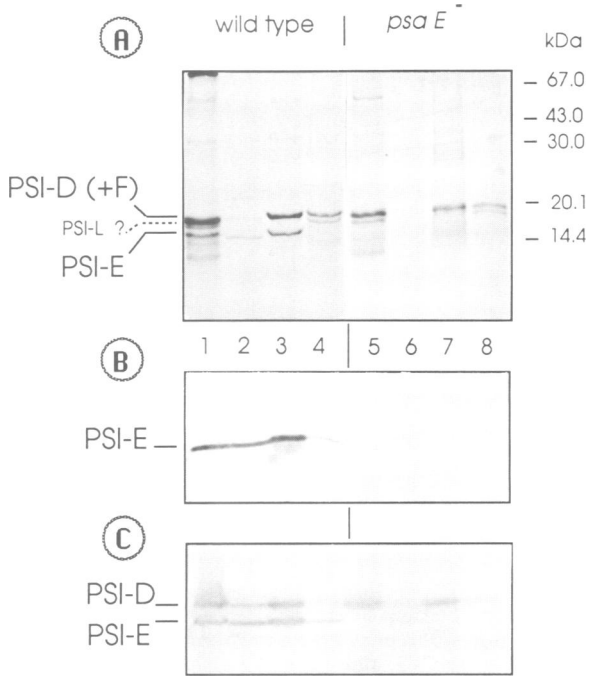

Fig. 3. Polypeptide composition of PSI from wild type and FKE_2 strains. PSI particles or various membrane fractions after NaSCN extractions were analyzed by SDS gel electrophoresis. Samples were precipitated in 80% cold acetone prior to solubilization in the sample buffer; loaded amounts of proteins correspond to 8 μg chlorophyll in the starting material. Proteins were visualized either by Coomassie blue staining (**A**) or by indirect detection by antibodies after electro-transfer on to a PVDF membrane (**B** and **C**). In this case, mouse polyclonal antibodies directed against PSI-E (B), or against PSI-E and PSI-D (C), were incubated overnight at 4°C at a 1/200 dilution. Bands were revealed using a second antibody coupled to alkaline phosphatase. Lanes 1 and 5 are control PSI from wild type or FKE_2^-; successively, 1 M NaSCN extracts of the membranes (lanes 2 and 6), 2 M NaSCN extracts (lanes 3 and 7) and the pellets after 2 M extraction (lanes 4 and 8) are analyzed. Experiments were run in parallel on the wild type (lanes 1–4) and the FKE_2 strain (lanes 5–8).

correctly deleted. Both DNAs from the wild type and the FKE_2 mutant were digested with *Hin*dIII or *Hin*cII. The fragments, separated by electrophoresis, were probed after Southern blotting with the digoxigenin-labeled *Eco*RI–*Bam*HI fragment from pFBsE including the *psaE* gene. The original *Hin*dIII band of the wild type was found at ~5.3 kbp (Figure 2, lane 1), in agreement with previously published information (Chitnis *et al.*, 1989b). This band is no longer present in the mutant (Figure 2, lane 3). In fact, insertion of the Km^r cassette introduced a new *Hin*dIII site, resulting in the appearance of two fragments at ~3.4 and 2.5 kbp. In a parallel experiment, DNA from the mutant was overloaded 15 times; even in this case, no traces of the original wild type fragment at 5.3 kbp was detected (data not shown). The unique *Hin*cII fragment of the mutant is located at ~4.8 kbp compared with the original 4.1 kbp (Figure 2, lanes 4 and 2). This is actually the expected size increase of 0.7 kbp for this fragment in the FKE_2 strain [+ Km^r cassette (1252 bp) − *psaE* deletion (535 bp) = +697 bp]. Therefore, we conclude that the selected mutant FKE_2^- no longer carries any *psaE* copy in its genome.

Biochemistry. PSI particles were purified from thylakoids of the wild type and FKE_2 mutant strain as described in Materials and methods. PSI polypeptides were then analyzed by denaturing electrophoresis using direct protein staining and also probing by antibodies specific for PSI-E or PSI-D. Prior to solubilization, samples were precipitated in cold 80% acetone; this treatment prevents the front smear due to the pigments but irreversibly aggregates the large subunits of PSI (PSI-A and -B). Under these conditions, the main remaining bands of the samples are peripheral proteins of PSI. We also took advantage of the differential extraction properties of PSI subunits in the presence of different concentrations of the chaotropic agent NaSCN (Lagoutte and Vallon, 1992). This extraction procedure, which was directly performed on the full membranes, contributes to give a more substantial amount of information than simple electrophoresis of intact PSI. As can be seen from Figure 3A (lane 2), a 1 h extraction of wild type membranes with 1 M NaSCN releases a small amount of PSI-D and PSI-E polypeptides, clearly revealed by the sensitive immunological test (Figure 3B and C, lane 2). Using a 2 M concentration of NaSCN is far more efficient, completely extracting PSI-D and PSI-E (Figure 3A, lane 3), as corroborated by antibody probing of the supernatant and of the pellet (Figure 3B and C, lanes 3 and 4). PSI-C (lowest band, Figure 3A lane 1) is more difficult to detect by staining in the 2 M extract, but it was previously isolated and partly sequenced from a similar supernatant (Rousseau and Lagoutte, 1990). It must be noted that the apparent molecular mass of PSI-E in this gel buffer system is about twice the expected value. The 2 M pellet (lane 4) essentially includes PSI-F, as identified by microsequencing of the upper band present in this pellet, with no detectable PSI-D sequence. The band just below PSI-F is probably PSI-L, as documented by other authors (Li *et al.*, 1991b). The differential chaotropic extraction by NaSCN thus clearly discriminates between PSI-D and PSI-F, which otherwise are often superimposed. This procedure could also be a useful approach in testing the influence of specific amino acid substitutions on the association properties of PSI subunits. The same analysis on the mutant FKE_2

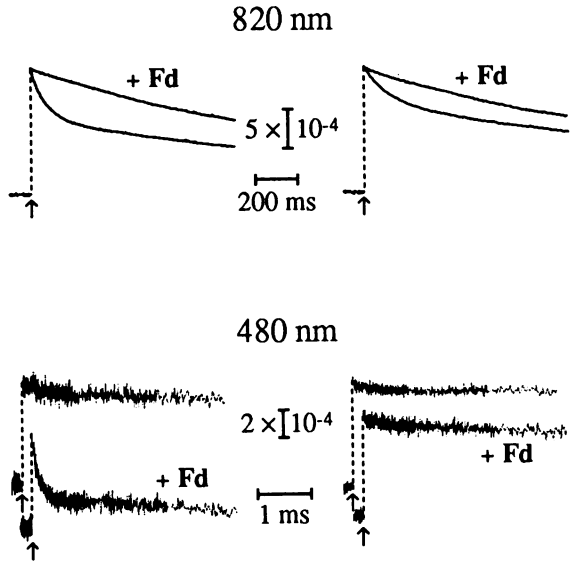

Fig. 4. Kinetics of absorption changes observed at 820 nm in isolated membranes (upper part) or at 480 nm in PSI particles (lower part) from *Synechocystis* 6803. Measurements were made at 293 K in the absence or presence of ferredoxin. Kinetics were induced by a saturating laser flash (wavelength = 694.3 nm; duration 6 ns; pulse energy 15 mJ; the repetition rate was 0.04 Hz for the upper curves and 0.125 Hz for the lower curves). Left part of the figure is for the wild type, and right part is for the *psaE*-deleted mutant. The membranes were suspended in 20 mM Tricine, pH 8, in the presence of 1 mM sodium ascorbate, 10 μM DPIP, 30 mM NaCl, 5 mM $MgCl_2$ and 0.03% β-DM. The PSI particles were suspended in 20 mM MOPS buffer, pH 7, in the presence of 4 mM sodium ascorbate, 75 μM DPIP, 30 mM NaCl, 5 mM $MgCl_2$ and 0.6% OGP; in the absence of ferredoxin, OD (optical density) = 1.85 for the membranes (upper curves) and OD (45°) = 1.65 for the PSI particles (lower curves) at the absorption maximum in the red region. The PSI concentration in the absence of ferredoxin is 0.25 μM (upper curves) and 2.57 μM (lower curves) (from ΔOD at 820 nm). When ferredoxin is present, its concentration amounts to 6.8 μM (upper curves) or 9.0 μM (lower curves). The absorption changes in the presence of ferredoxin were multiplied by the dilution factor due to ferredoxin addition for easy comparison of the kinetic traces. All measurements at 820 nm were made after prolonged degassing under vacuum. Each trace is the average of 16 experiments.

(Figure 3, lanes 5–8) confirmed the complete absence of the corresponding polypeptide. No other substitutive polypeptide of equivalent apparent molecular mass could be detected. Anti-PSI-E antibodies also failed to recognize the original polypeptide in the mutant (Figure 3B, lanes 5 and 7). PSI-D is still present in the mutant as detected by staining (Figure 3A, lanes 5 and 7), N-terminal microsequencing and also antibody binding (Figure 3C, lanes 5 and 7). However, the antibody signal seems to be reproducibly lower than in the wild type, with minor degradation products in the NaSCN extracts. This could reflect a higher susceptibility to proteolysis of the depleted PSI.

Some faint bands can also be observed in the intermediate molecular weight range above PSI-D. The relative amount of these secondary proteins differs slightly between the wild type and FKE_2 (Figure 3A, lanes 3 and 7), but they are not among the well characterized PSI subunits and are considered as minor contaminants.

Electron paramagnetic resonance spectroscopy (EPR). EPR signals of the different iron-sulfur centers were measured in PSI particles prepared either from the wild type or from the mutant lacking PSI-E. Under different conditions which are described immediately below, different types of signals were recorded, which were all identical in their g-values as well as in their magnitudes for the two types of PSI particles (see Sétif *et al.*, 1987 and Sétif and Bottin, 1989 for similar signals recorded in wild type PSI particles).

EPR samples prepared in the presence of ascorbate and dichlorophenolindophenol (DPIP) at pH 8 were frozen in the dark. Illumination at 15 K induced an irreversible charge separation which resulted in the state [$P700^+$ – ($Fe\text{-}S_A$, $Fe\text{-}S_B$)$^-$]. Assessment of photochemistry at 15 K was thus evaluated by measuring a difference spectrum (after illumination minus before illumination). The g-values, as well as the absolute amounts of $Fe\text{-}S_A^-$ and $Fe\text{-}SB^-$, were indistinguishable in the wild type and in the mutant.

EPR samples were also prepared at pH 10 in the presence of an excess of sodium dithionite. In a first series of experiments, the samples were frozen in the dark, allowing the detection at 15 K of EPR signals which corresponded to a redox state where both $Fe\text{-}S_A$ and $Fe\text{-}S_B$ are reduced. The signals due to ($Fe\text{-}S_A^-$, $Fe\text{-}S_B^-$) were identical in both cases. In a second series of experiments, the samples were illuminated with a strong light intensity at room temperature and were thereafter illuminated during freezing. Such a treatment allows the iron-sulfur center $Fe\text{-}S_X$ (which is the third iron-sulfur center present in PSI) to be reduced completely, in addition to the centers $Fe\text{-}S_A$ and $Fe\text{-}S_B$. Signals of $Fe\text{-}S_X^-$, which were detected at 10 K, were also identical in both cases.

Flash-absorption spectroscopy. In PSI complexes, the primary photoinduced charge separation is normally followed by electron transfer along a chain of electron acceptors. This process leads eventually to the formation of the oxidized primary donor $P700^+$ on one hand and of the reduced terminal acceptor (either $Fe\text{-}S_A^-$ or $Fe\text{-}S_B^-$) on the other hand. In the absence of soluble partners for electron transfer, the charge separation is generally thought to be followed by a recombination reaction between $P700^+$ and ($Fe\text{-}S_A$, $Fe\text{-}S_B$)$^-$. Such a recombination can be observed in the upper half of Figure 4, where $P700^+$ is monitored at 820 nm in isolated membranes. However, this rapid recombination amounts only to ~45 and 30% of the total absorption decay respectively in the wild type and in the mutant lacking PSI-E. The remaining part of the absorption change decays much more slowly and can be ascribed to the reduction of $P700^+$ by the exogenous donor $DPIPH_2$ in PSI where an electron has escaped from ($Fe\text{-}S_A$, $Fe\text{-}S_B$)$^-$. Which species oxidizes ($Fe\text{-}S_A$, $Fe\text{-}S_B$)$^-$ is unknown at the moment, but it appears that dissolved oxygen can be excluded, as these measurements were made under vacuum after severe degassing of the samples. From complementary experiments, it can be concluded that the biphasic character of the kinetics described above is not due to some kinetic heterogeneity of PSI but can be ascribed to some competition between the recombination and escape processes.

In the presence of ferredoxin (6.8 μM for a PSI concentration of 0.25 μM), the two decay curves at 820 nm corresponding to the wild type and to the mutant become indistinguishable (Figure 4). For both types of membrane, addition of soluble ferredoxin abolishes almost entirely the faster decay due to the recombination reaction, which then amounts to <5% in both cases. This observation can easily

be interpreted by assuming that ferredoxin is reduced with a yield close to 100% by (Fe-S_A, Fe-S_B)$^-$, at least in the PSI complexes undergoing a recombination reaction in the absence of ferredoxin. It thus appears that addition of ferredoxin has the same effects on the $P700^+$ decay in the wild type and in the mutant lacking PSI-E.

In a second set of experiments, we directly recorded the reduction of ferredoxin by PSI particles at wavelengths where the differential absorption coefficients (oxidized minus reduced) of (Fe-S_A, Fe-S_B) and ferredoxin are different. This condition is fulfilled in the wavelength region between 460 and 600 nm, where electron transfer from (Fe-S_A, Fe-S_B)$^-$ to ferredoxin should be accompanied by a negative absorption change. Flash-induced absorption changes have been measured in this spectral region and agree fairly well with the calculated spectrum corresponding to this reaction (P.Sétif, unpublished observations). In the following, kinetics of absorption changes are shown at 480 nm. This wavelength is particularly convenient as it corresponds both to large absorption changes for ferredoxin reduction and to the isobestic point of carotenoid triplet states in these PSI particles (P.Sétif and R.Delosme, unpublished results). The results of such experiments at 480 nm are shown in the lower half of Figure 4, where kinetics were recorded in the absence or presence of ferredoxin. The fast positive absorption change which is observed immediately after the laser flash is primarily due to the formation of $P700^+$, as reduction of (Fe-S_A, Fe-S_B) is associated with a very small contribution at this wavelength (Ke, 1973). In the absence of ferredoxin, the signal at 480 mn is fairly stable during the first 4 ms, as would be expected for a signal due essentially to $P700^+$. After addition of ferredoxin (9 μM for a PSI concentration of 2.2−2.6 μM), PSI particles from the wild type and from the mutant exhibit a very different kinetic behavior. Addition of ferredoxin has little effect in the case of the mutant, but gives rise to an important fast decrease in the case of the wild type. This decay exhibits two different components ($t_{1/2}$ 80 μs and 400 μs). The faster one is related to an absorption change whereas the slower component is probably due to a flash-induced scattering change (P.Sétif, unpublished observations; see Materials and methods). The amplitude of the 80 μs decay can be calculated to amount to ~40% of what is expected for electron transfer from (Fe-S_A, Fe-S_B)$^-$ to ferredoxin in 100% of the PSI complexes. The possible origins of this deficit in amplitude are under investigation. Though not proven yet, the most likely interpretation is that in 60% of the PSI complexes the reduction of ferredoxin is slower, so that reduced ferredoxin cannot accumulate due to some reoxidation process (with $t_{1/2} > 1$ ms). As the kinetics of ferredoxin reduction become faster when the concentration of ferredoxin is increased (not shown), the 80 μs phase must be at least partially diffusion-limited. Assuming a second-order process for the whole decay (corresponding approximately to a pseudo-first order reaction, as ferredoxin is in excess compared with PSI), a second order rate constant of $\sim 10^9$ M^{-1} s^{-1} can be calculated.

In the deleted mutant FKE_2, a small difference is observed between the two decay kinetics in the absence or presence of ferredoxin (Figure 4, lower right). It might also be related to some ferredoxin reduction, though it was too small for a precise spectral and kinetic characterization. It thus appears that only a small amount of reduced ferredoxin

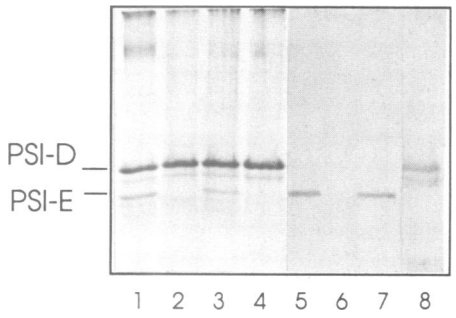

Fig. 5. Polypeptide composition of reconstituted PSI samples. PSI particles from $pFKE_2$ strain were reconstituted with purified PSI-E polypeptide from *Synechocystis* 6803 or spinach. Proteins were either stained with Coomassie blue (lanes 1−4) or detected by specific antibodies after electrotransfer on to a PVDF membrane (lanes 5−8). A mixture of monoclonal antibodies (Lagoutte and Vallon, 1992) was used at a 1/2000 dilution to detect the spinach E subunit. Successive samples are the following: wild type PSI (lanes 1 and 5), mutant PSI (lanes 2 and 6) and mutant PSI reconstituted with either *Synechocystis* subunit (lanes 3 and 7) or spinach subunit (lanes 4 and 8).

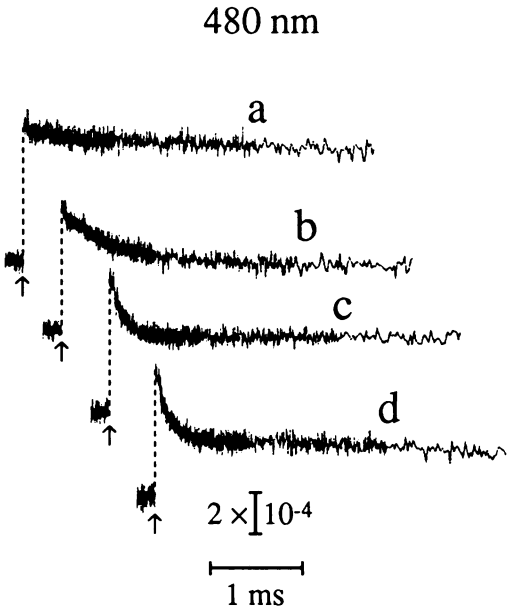

Fig. 6. Kinetics of absorption changes measured at 480 nm in the presence of 9.0 μM ferredoxin in different PSI particles from *Synechocystis*. Other conditions are similar to those described in Figure 4 for the measurements at 480 nm. Trace **a**: mutant lacking subunit PSI-E. Trace **b**: same mutant reconstituted with PSI-E subunit from spinach. Trace **c**: same mutant as in trace a reconstituted with PSI-E subunit from *Synechocystis*. Trace **d**: wild type PSI particles. Optical densities measured at 679 nm (absorption maximum) at 45° were respectively 1.50, 1.49, 1.54 and 1.50. PSI concentration (from ΔOD at 820 nm) were respectively 2.34, 2.32, 2.39 and 2.34 mM. Each trace is the average of 16 experiments.

(at most a concentration corresponding to 10% of the PSI concentration) can be detected at 480 nm after laser flash excitation of the PSI particles from FKE_2. Although we deduced from the preceding experiment at 820 nm that ferredoxin fully inhibits the back-reaction between $P700^+$ and (Fe-S_A, Fe-S_B)$^-$, this nearly complete absence of decay at 480 nm shows that no or little reduced ferredoxin can accumulate. This is presumably due to a reoxidation of reduced ferredoxin competing more efficiently with the reduction process in the mutant PSI. The chemical identity

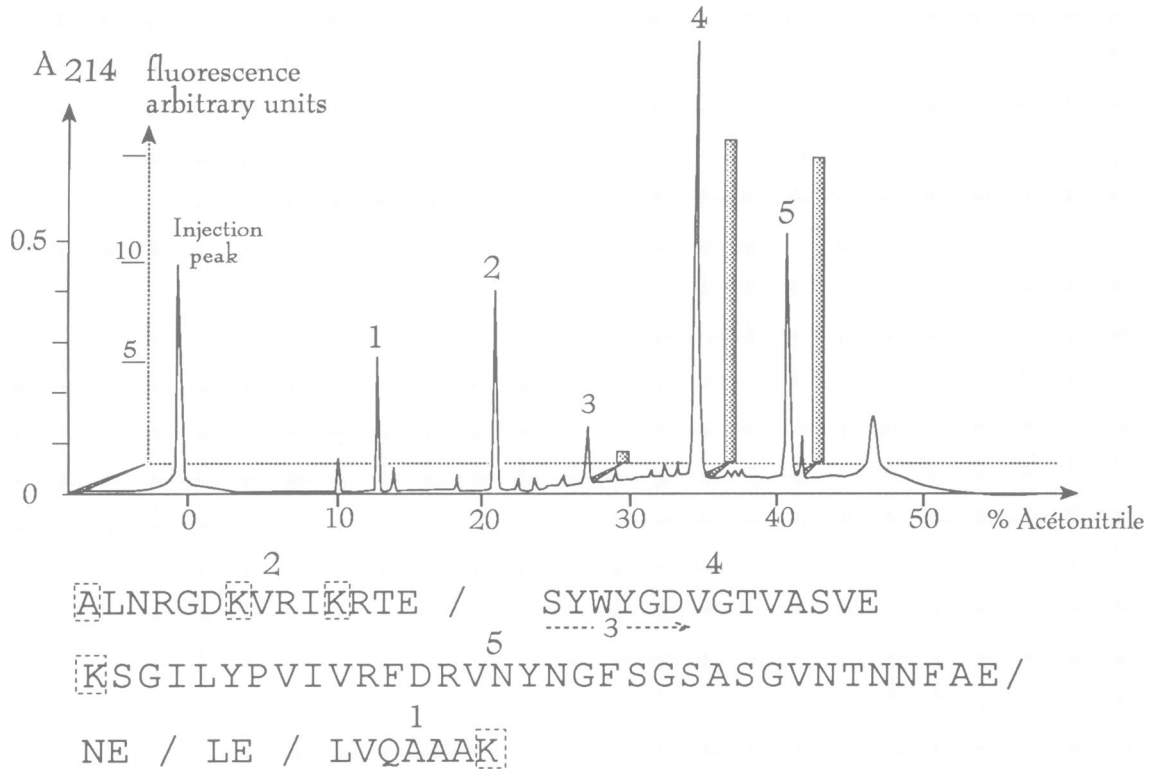

Fig. 7. Elution pattern of the polypeptides obtained after glutamic cleavage of FITC-labeled PSI-E. Purified PSI-E was subjected to proteolytic cleavage using the V8 enzyme under conditions where it mainly cleaves after glutamic residues. The mixture of polypeptides was resolved by reversed phase chromatography on a C18 Delta-pak column eluted with an acetonitrile gradient in TFA/H_2O (0.1%, v/v), at a flow rate of 1.0 ml/min. The front chromatogram is the peptide elution pattern recorded at 214 nm. The bar plot at the back is the total fluorescence of each peptide measured at 515 nm with an excitation at 470 nm. Slashes in the sequence are at the main cleavage sites. Amino acids in boxes are the most classical targets for Edman-type reagents.

of the species responsible for the oxidation of reduced ferredoxin is not clear at the moment, as oxygen is not the only possible partner in this process. If correct, the preceding interpretation places a lower limit on the halftime of ferredoxin reduction in the absence of PSI-E: assuming a halftime of ferredoxin reoxidation similar to that of the wild type ($t_{½} > 1$ ms), the $t_{½}$ for ferredoxin reduction in the mutant should be > 2 ms. On the other hand, this halftime should be < 10 ms in order to account for the very efficient inhibition of the recombination reaction between $P700^+$ and $(Fe\text{-}S_A, Fe\text{-}S_B)^-$. Therefore, under the experimental conditions corresponding to the data of Figure 4, the halftime of ferredoxin reduction in the mutant should be between 2 and 10 ms (rate between 70 and 300 s^{-1}).

Reconstitution experiments

From the preceding results, the PSI-E polypeptide appears to be necessary for fast submillisecond electron transfer from PSI to soluble ferredoxin. In order to confirm this role and to check the absence of side effects of PSI-E deletion on other PSI components, we tried to reconstitute the deficient PSI particle. When analyzed by electrophoresis, a deficient PSI reconstituted with the homologous PSI-E subunit exhibits an amount of reassociated protein similar to that of the wild type PSI (Figure 5, lanes 1 and 3). Migration of the polypeptide was the same, and probing with antibodies confirmed the identity of this electrophoretic band (Figure 5, lane 7). The efficiency of electron transfer to ferredoxin was investigated in this reconstituted particle (Figure 6). The signal of ferredoxin reduction was recorded at 480 nm; it originally exhibited the two fast components described above ($t_{½} \approx 80$ μs and 400 μs). The slower one (light-induced scattering; see Materials and methods) was subtracted from the original signals in these experiments, so that only the real absorption changes can be compared between different reconstituted samples. The transient absorption decrease recovered after homologous reconstitution (Figure 6c) appears very similar to that observed in the wild type PSI (Figure 6d) (same amplitude, $t_{½} \approx 90$ and 80 μs respectively). This experiment shows that PSI-E deletion results in fully reversible effects in the PSI, at least considering the fast reduction of ferredoxin.

We also tentatively reconstituted the same deficient PSI with a purified polypeptide from spinach. Unfortunately, this PSI-E subunit has the same electrophoretic mobility as the PSI-D subunit from *Synechocystis* (Figure 5, lane 4). It was thus difficult in this case to ascertain the yield of reconstitution by protein staining, but probing with antibodies clearly detected the presence of a substantial amount of the subunit in PSI (Figure 5, lane 8). Some degradation of the spinach subunit seems to occur in this heterologous PSI complex, a degradation which was not observed in the starting sample of the purified subunit. When looking at the ferredoxin reduction (Figure 6b), a transient absorption decrease is also observed, but with a 40% diminution of the amplitude and an increase of the $t_{½}$ up to 320 μs. In spite of the large extra N-terminal sequence present in the spinach PSI-E (30 amino acids), this polypeptide is capable of binding to the cyanobacterial PSI and of partly restoring fast ferredoxin reduction.

Table I. Different site-directed mutagenesis of PSI-E, and their effect on the integration of the subunit into PSI (±) and the fast reduction of ferredoxin (±)

		PSI-E protein in PSI	fast reduction of ferredoxin	
WT	...R..K.R.K R...Y W Y--K--LELVQAAAK (4 7 9 11 12 16 17 18 29 65)	+	+	WT
FCE1	A N	+	+	FCE1
FCE2	N E A	−	−	FCE2
FCE3	A	+	+	FCE3
FCE4	A N A	−	−	FCE4
FCE5	A	+	+	FCE5
FCE6	F F	+	+	FCE6
FCE7	A	+	+	FCE7
FCE8	Stop	−	−	FCE8

Site-directed mutagenesis of psaE

In a first search for PSI-E sequences exposed to the aqueous phase and thus possible candidates for interaction with soluble partners, we tried to label accessible primary amines with the fluorescent probe fluorescein isothiocyanate (FITC). Like Edman's reagent, FITC reacts readily with alpha amino groups but also occasionally with some of the most accessible epsilon amino groups of lysines. This has been found to be the case for one accessible lysine in the membrane calcium ATPase (Mitchinson *et al.*, 1982). On this basis, a similar reaction was performed on a full membrane fraction after extensive washing of the phycobilisomes. PSI-E protein was then purified as described, and its absorption spectrum was recorded. Apart from the UV absorption near 280 nm, partly due to the protein itself, a large visible absorption peak at 495 nm was attributed to the bound FITC, with the characteristic red shift of ~6 nm compared with the free reagent (489 nm) (Tietze *et al.*, 1962; Pick and Karlish, 1980). This labeled PSI-E subunit was then cleaved after glutamic residues by V8 protease and the resulting peptides were separated by reversed phase chromatography. As expected from the sequence, the elution pattern is quite simple, with four major peaks (Figure 7). All four peptides were completely sequenced and their fluorescence recorded. Peptides 1 and 2 were respectively identified as the C- and N-terminal ends. They are probably shielded from the reaction medium as evidenced by the total absence of fluorescence, despite having a binding potentiality of respectively 1 and 3 residues. Peptide 5 is the largest, covering the central part of the protein; fluorescence associated with this peptide is probably due to the labeling of the unique lysine of its N-terminal end. Unfortunately, it was not possible to detect clearly the fluorescent lysine derivative after automatic Edman degradation, excluding a direct determination of the labeled amino acid. Of special interest is peptide 4, which exhibited the same level of fluorescence as peptide 5 relative to the N-terminal amount; this was indicative of a comparable labeling of both peptides. No lysine is present in this peptide, and non-covalent binding of FITC is excluded at this step of the purification. As yet we have no clear explanation of this binding, which may be due to a side reaction of the isothiocyanate (Drobnica *et al.* 1977). The N-terminal end of peptide 4 seems to be involved in this binding as a small fluorescence was associated with the minor peptide 3 (S-Y-W-Y-G-D), a peptide resulting from an additional cleavage after aspartic 20. Whatever the explanation for this second binding site

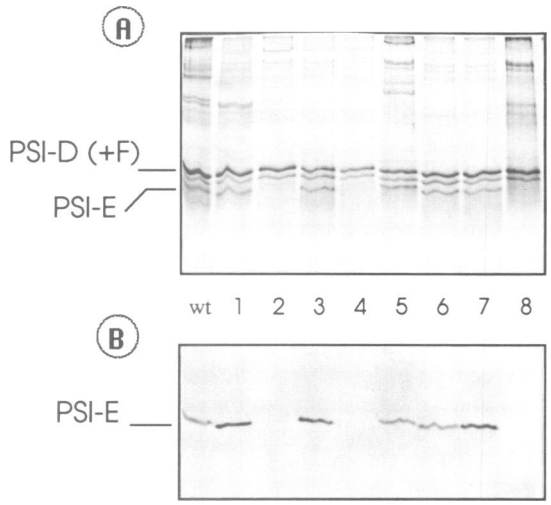

Fig. 8. Polypeptide composition of PSI from *psaE* mutants. PSI samples from the different mutants were prepared as described in Figure 3. Proteins were either stained with Coomassie blue (**A**) or detected by anti-PSI-E antibodies after electro-transfer on a PVDF membrane (**B**). wt is for the control wild type PSI, and PSI from the various mutants are numbered from 1 to 8 as in the text and Table I.

is, it appears that a central region of PSI-E, starting possibly at serine 15 and extending at least to lysine 29, is partly accessible to the stroma, whereas neither the N- nor the C-terminal end is.

This structural information guided site-directed mutagenesis of the *psaE* gene, which can be classified in two main series. In a first series of experiments, we modified the N- or C-terminal ends of the sequence. As these parts of PSI-E, which are supposedly shielded, are good candidates for interactions with other components of PSI, we examined the effect of strong perturbations of these sequences on the integration properties of the subunit. The very basic charge of the N-terminal was more or less dramatically modified in mutants 1 to 4 (Table I). The most drastic change was in mutant FCE2, where an acidic and two neutral amino acids have replaced three basic residues. The C-terminal from residue 60, which also seems to be buried in the complex, has the only helix-forming potentiality (Rousseau and Lagoutte, 1990). This end of the molecule was partly suppressed in mutant FCE8 by introducing a stop codon instead of leucine 65. The central accessible part of the protein was modified in a less drastic way. The tryptophan

in the tripeptide Y_{16}-W_{17}-Y_{18} was changed to an alanine (FCE5) which is known to be a neutral amino acid with respect to protein structure. The two tyrosines were also replaced by two phenylalanines (FCE6) to keep the possible interactions of aromatic rings without the effect of hydroxyl groups. Finally, the only lysine residue accessible to FITC (K_{29}) was changed to an alanine (FCE7).

The Bluescript plasmids used for mutagenesis were all derived from pFBsCE; they were numbered from 1 to 8. Three of the modified sequences incorporated a new restriction site, allowing a simple selection of the mutated plasmids. Sequencing of all selected plasmids was systematically performed. Transformants were selected after five rounds of streaking on chloramphenicol plates and further grown in liquid cultures, always in the presence of the antibiotic. The strain FKE_2, which has the *psaE* gene completely deleted, was used for all these transformations. A major advantage of this two-step protocol, based first on a gene deletion, is that one can be sure that all expressed proteins are mutated ones, even if the final recovered set of mutated copies is not complete.

Three mutants, FCE2, FCE4 and FCE8, failed to incorporate the PSI-E subunit, as judged from direct protein staining (Figure 8A). Probing with specific antibodies confirmed that no other immunologically related polypeptide is present in these three mutants (Figure 8B). All other mutants exhibited a normal amount of PSI-E, although the relative migration of this protein is slightly modified in the case of FCE5. When analyzed for their ability to efficiently transfer electrons to ferredoxin, the mutants lacking PSI-E (FCE2, 4 and 8) were similar to the deleted strain, FKE_2. On the other hand, all mutants having incorporated a modified PSI-E behaved similarly to the wild type, the reduction of ferredoxin proceeding with halftimes comprised between 80 μs and 120 μs (see Table I). Changing tryptophan 17 or lysine 29 to alanine (FCE5 and FCE7) did not significantly affect electron transfer to ferredoxin. The same was observed for FCE6, in which tyrosines 16 and 18 were both replaced by phenylalanines. All these modifications were expected to be essentially neutral at the structural level, without consequences on the integration of the polypeptide, as they are located on the predicted outside part of the protein (FITC labeling). Insertion in PSI complex was effectively preserved but also a fast electron transfer to ferredoxin (Table I). Further studies will be necessary to determine if more subtle changes in the electron transfer properties to ferredoxin can be found in the different mutants which have incorporated a modified PSI-E subunit.

Discussion

Up to now, it has not been possible to assign any precise function to the PSI-E subunit, though a role in binding FNR has recently been proposed in the case of barley (Andersen *et al.*, 1992). Many different sequences of this protein have been described, all of which exhibit a high degree of conservation. Higher plants have an extra N-terminal sequence, ~30 amino acids long, as compared with cyanobacteria; the sequence identity for the common C-terminal region is 60% (Golbeck, 1991). Between cyanobacteria, this identity rises to 73%, a higher score than that found for PSI-D (65%). This high level of conservation is indicative of an essential role of PSI-E at the interface between the PSI complex and the stroma. In contrast with the lack of functional information, the location of PSI-E on the stromal side of the membrane has been substantiated by different experimental approaches (Bengis and Nelson, 1977; Ortiz *et al.*, 1985). This location was also inferred from sequence information (Münch *et al.*, 1988; Okkels *et al.*, 1988; Franzen *et al.*, 1989). Other studies made on eukaryotic PSI complexes also showed that PSI-E is in close interaction both with PSI-C, which carries the iron-sulfur centers Fe-S_A and Fe-S_B, and with PSI-D (Oh-oka *et al.*, 1989). More precise topological information was also recently obtained for spinach PSI-E (Lagoutte and Vallon, 1992). In this case, two different regions were predicted to be accessible in the native system: a central region and a region comprising at least the 15 N-terminal amino acids. We have shown in the present work that the N-terminal end of PSI-E, which is shortened in *Synechocystis* 6803, is probably not accessible to the stroma. The C-terminus seems also to be shielded, as in spinach: the only sequence accessible for *in situ* labeling by FITC is in the middle part of the protein. Therefore, we postulate that both ends of PSI-E could interact with other PSI proteins. In favor of these conclusions, drastic mutations located on these terminal ends result in a lack of integration of the subunit in PSI, which is not the case for modifications of what is supposed to be a stroma-accessible region. Of particular interest is the intricate set of basic amino acids that seems to be required at the N-terminal end for the correct binding of the subunit. The suppression of one positive charge (arginine 12 in FCE3), or even two positive charges (lysines 7 and 11 in FCE1) impaired neither PSI-E binding nor its role in ferredoxin reduction, whereas the suppression of arginine 12 in combination with two other basic residues (FCE2 and FCE4) prevented this binding. The effect of symmetrical modifications of potential acidic counterparts on other subunits will give valuable information on possible sites of interaction of PSI-E.

Concerning spectroscopic and functional properties, our results show that the PSI particles prepared from the *psaE*-deleted mutant exhibit an important decrease in the rate of ferredoxin reduction compared with the wild type, though the other properties that we have determined are very similar in both types of PSI particle. Considering the characteristics of the PSI itself, our observations are in full agreement with a previous study on a partly reconstituted PSI particle (Li *et al.*, 1991a). In that study, PSI cores (without PSI-C, PSI-D and PSI-E) were reconstituted with just PSI-C and PSI-D proteins under conditions where the iron-sulfur centers are rebuilt. PSI particles recovered in this way (minus PSI-E) were indistinguishable from the original control PSI particles. A previous study made on the same cyanobacterial strain (*Synechocystis* PCC 6803) indicated that the photoautotrophic growth was not affected by deletion of the *psaE* gene (Chitnis *et al.*, 1989b). The PSI activity, measured as the cellular oxygen uptake when PSII is blocked, was also measured to be ~70% that of the wild type when normalized to the amount of chlorophyll. However, the chlorophyll to P700 ratio in PSI particles as well as in thylakoids was larger for the mutant than for the wild type so that the PSI activity can be calculated to be almost unchanged when normalized to the P700 content. In contrast with these results, we did not find any difference in the chlorophyll to P700 ratio in our PSI preparations. The growth of our deleted strain,

which was conducted under strict photoautotrophic conditions, also showed no significant difference from the wild type growth.

Both the genetic and spectroscopic experiments presented in this work provide the first clear and direct evidence for a functional role of a peripheral PSI subunit (PSI-E) in the interaction between PSI and soluble ferredoxin. Under the experimental conditions depicted here, the yield of ferredoxin reduction by PSI is probably not significantly affected by PSI-E depletion whereas the rate of this process decreases by a factor of a least 25. Moreover, PSI particles prepared from the *psaE*-deleted mutant completely recovered their capacity to reduce ferredoxin rapidly when purified PSI-E polypeptide was added back to the system. The rate of ferredoxin reduction that we observe in the presence of PSI-E is much larger than the rates that have been measured recently with Triton solubilized spinach particles (Hervas *et al.*, 1992) (8600 s^{-1} versus 140−180 s^{-1}). These discrepancies may be due to the use of different starting biological materials or to the use of different detergents. In the last hypothesis, this could mean that Triton has deleterious effects on the stromal side of PSI complexes, which result in some modification in the interaction with soluble ferredoxin.

The important role of PSI-E in the PSI−ferredoxin interaction was unexpected after the results of cross-linking experiments, since only PSI-D was bound to ferredoxin using EDC reagent (Zanetti and Merati, 1987; Zilber and Malkin, 1988). Several possible explanations can be proposed for this apparent discrepancy, which should be tested in future work. One possibility is that PSI-E may be part of the docking site for ferredoxin but cannot be cross-linked to ferredoxin due to the nature of the interaction or due to the distance separating the different partners, as EDC is a zero-length cross-linker. Several other bifunctional reagents still need to be tested to clarify this point. Alternatively, PSI-E may have only an indirect role if it is not part of the docking site by itself. In that case, its absence could modify the interaction between PSI-D and ferredoxin. This indirect effect may have several origins, e.g. the unmasking of wrong docking sites or a structural modification of PSI-D in the absence of PSI-E. As both ends of PSI-E seem to interact inside the complex, one can imagine a bridging effect, keeping the right distances and conformations between other components of the system. More complete site-directed mutagenesis will help to answer this important question.

Materials and methods

Materials

Most of the molecular biology reagents and enzymes were from Pharmacia, New England Biolabs and Boehringer Mannheim. The digoxigenin labeling kit and the fluorescent reagent 3-(2′-spiroadamantane)-4-methoxy-4-(3′′ phosphoryloxy)-phenyl-1,2-dioxetane (AMPPD) were from Boehringer Mannheim. Site-directed mutagenesis was following the procedure of Bio-Rad using the *Escherichia coli* strain CJ236. The chloramphenicol resistance gene (*cam*^{r}) was isolated from plasmid pLF8, a gift from Dr F.Chauvat (Labarre *et al.*, 1989), providing a 1252 bp resistance cassette (Cm^r). The kanamycin resistance gene (*kan*^{r}) was from transposon Tn *903* (Pharmacia) and was used as a 1300 bp resistance cassette (Km^r). An anti-mouse antibody coupled to alkaline phosphatase was from Promega Biotech and polyvinylidene difluoride (PVDF) membrane for protein transfer was from Millipore. [^{35}S]dATP for sequencing was from Amersham. Most classical chemicals were from Sigma or Merck. All DNA sequences were analyzed with the DNA Strider software (Marck, 1988).

DNA isolation and hybridization

Genomic DNA from liquid cultures of *Synechocystis* sp. PCC 6803 was isolated as previously described (Tandeau de Marsac *et al.*, 1982) and purified on Quiagen pack (Quiagen Inc.). Southern hybridization was performed using 2 μg DNA for each restriction digestion. DNA fragments were electrophoresed on 0.8% agarose gel and transferred to Hybond-N membrane (Amersham) using a vacuum transfer system. The *Eco*RI−*Bam*HI insert of the plasmid pFBsE, including the *psaE* gene (see Results), was used as a template for random priming with digoxigenin dUTP analog. The resulting labeled mixture was directly used as a probe, following the recommended detection procedure (Boehringer).

PCR amplification

The strategy for cloning *psaE* started with a PCR procedure based on the previously published sequence of *Synechocystis* 6803 (Chitnis *et al.*, 1989b). The first oligomer, complementary to the coding strand, was designed to introduce a *Bam*HI restriction site 780 bp upstream of the starting ATG. This was achieved by a point mutation (G to A) at the third position of the site: CCGCCAAGTTGGGATCCTGGCGTAGGGAC. The second oligomer was complementary to the non-coding strand. In this case, a new *Eco*RI site was introduced 520 bp downstream of the coding sequence also by a point mutation (T to A) at the third position of the restriction site: GGGCGGCGACTGGAATTCAGCTTTTCGTAG. The optimum conditions for amplification were obtained by using 1 μg of total genomic DNA and 2 U of *Taq* polymerase (Pharmacia) at final concentrations of 5 mM magnesium, 200 μM of each dNTP and 1 μM of each oligomer (total volume 100 μl).

DNA sequencing

Sequencing was by the dideoxy termination method (Sanger *et al.*, 1977); double-stranded Bluescript DNA was first denatured by the alkaline procedure (Chen and Seeburg, 1985).

Culture conditions

Cells of the wild type and mutants were grown in BG11 medium (Rippka *et al.*, 1979), buffered with 6 mM HEPES, pH 7.3. Solid cultures were on 1.5% agar plates; in this case, HEPES buffer was omitted from BG11. Transformation (Chauvat *et al.*, 1986) was done with plasmid DNA from the Bluescript SK$^+$ vector. 50 ml of BG11 were inoculated with wild type cells from a culture in the logarithmic phase of growth. This second liquid culture was allowed to reach 1 absorbance unit at 580 nm. After two washes with fresh culture medium, the cells were resuspended in 5 ml of the same medium and 1 μg of plasmid transformant DNA was added. Transformation proceeded up to 90 min at 34°C under 3500 lux illumination. 100 μl aliquots of the cell suspension were spread directly on agar plates and allowed to grow for 24 h under dim light. Transformant selection started by establishing an antibiotic gradient through the agar. This was achieved by adding 0.4 ml of the appropriate antibiotic underneath the agar and by gently lifting it from the Petri dish. Antibiotic concentrations in the starting solutions were of 5 mg/ml for kanamycin and of 1 mg/ml for chloramphenicol. Transformed colonies were then segregated by five successive replicates on agar plates in the presence of either kanamycin (50 μg/ml) or chloramphenicol (10 μg/ml).

Thylakoid and PSI isolation

Cells were harvested at the late log phase of growth, resuspended in 50 mM Tricine pH 7.5, 10 mM KCl, 1 mM EDTA and 0.2 mM each of PMSF, aminocaproic acid and benzamidine), and disrupted three times in a French pressure cell at 20 000 lb/in^2. The homogenate was centrifuged for 10 min at 12 000 *g*. The resulting supernatant was diluted in the same buffer and the small thylakoid fragments were recovered by centrifugation at 200 000 *g* for 1 h. After two rounds of washing under the same conditions, the buffer was changed for 25 mM Tris−HCl pH 8.0, 1 mM EDTA and the PSI was solubilized at a concentration of 1 mg/ml by a mixture of octyl-β-D-glucopyranoside (OGP) and sodium cholate as previously described (Bottin and Sétif, 1991). This procedure leads to a multimeric form of PSI which can be recovered by pelleting at 200 000 *g* for 2 h.

Purification of proteins

PSI-E polypeptide from spinach was purified by a differential chaotropic extraction of the thylakoid membranes, followed by a two-step chromatographic procedure as recently described (Lagoutte and Vallon, 1992). A similar protocol has been applied to photosynthetic membranes of *Synechocystis*. In this case, the first extraction with 1 M NaSCN was omitted as it did not improve the purification and sometimes resulted in some release of PSI-E. The 2 M NaSCN extract, which is essentially a mixture of PSI-D, PSI-E and PSI-C (see Results, Figure 3), was first purified

by filtration on a TSK 2000 column (LKB). The following reversed phase chromatography was run on a C18 Delta-pak column (Waters) using a linear acetonitrile gradient in TFA/H_2O (0.1%, v/v). The flow rate was of 1 ml/min and the acetonitrile increase was of 2% per ml. Under these conditions, PSI-E and PSI-D subunits eluted very close, in this order, near 60% acetonitrile. Ferredoxin from *Synechocystis* was a gift from Dr H.Bottin (Bottin and Lagoutte, 1992).

Protein labeling

The fluorescent probe fluorescein isothiocyanate (FITC) was used to label accessible primary amines (mainly N-terminal ends of polypeptide chains and also some epsilon amino group of lysines). Membranes collected just before the PSI solubilization step were used in this experiment after two additional washes in 50 mM borate buffer, pH 9.3. The last pellet was resuspended in the same buffer at a final chlorophyll concentration of 0.5 mg/ml, and FITC was added to a final concentration of 1 mg/ml. The reaction was allowed to proceed at room temperature for 1 h. Preliminary experiments showed that such a reaction time was sufficient to reach a plateau of fluorescence binding to PSI-E and PSI-D.

Reconstitution experiments

PSI particles from the *psaE* minus mutant were diluted to 0.1 mg chlorophyll/ml in 50 mM Tris buffer pH 8.5, 1 mM EDTA; purified PSI-E from either *Synechocystis* or spinach was then added at a 10-fold molar excess over PSI. Reassociation was allowed to proceed at 22°C for 1 h, and PSI was recovered after two rounds of washing and centrifugation at 200 000 *g* (2 h).

Electrophoresis

Mini slab gel electrophoresis (Bio-Rad apparatus) was used for protein characterization. Gel buffers, sample buffer and acrylamide to bisacrylamide ratio were as described by Laemmli (1970), with final acrylamide concentrations of 6% in the stacking gel and 15% in the resolving gel. SDS was omitted from the gels. Anode buffer was 0.2 M Tris–HCl, pH 8.9 and cathode buffer was 0.1 M Tris, 0.1 M Tricine, 0.1% SDS, resulting in a pH of 8.25 as described by Schägger and Von Jagow (1987). For antibody probing, gels were transferred electrophoretically on to PVDF membranes (Immobilon P from Millipore) as described by Lagoutte and Vallon (1992).

Immunization

Immunization of mice with PSI-D or PSI-E was following a classical three-step injection protocol. Ascitic fluids were obtained after intraperitoneal injection of Erlich cells; they were directly used at a dilution of 1/200 for probing Western blots.

Biophysical measurements

Low temperature EPR measurements were performed at 10 or 15 K with a Bruker ESR 200 X-band spectrometer equipped with an Oxford Instruments cryostat. The different samples (PSI particles from either the wild type or the *psaE*-deleted mutant) were put into calibrated quartz tubes at a chlorophyll concentration of 1 mg/ml. The redox and light treatments were standard and can be found elsewhere (Sétif *et al.*, 1987; Sétif and Bottin, 1989).

Flash-induced absorption changes were recorded at room temperature at two different wavelengths (480 and 820 nm) with a microsecond time resolution. The sample was analyzed either in a square cuvette (1×1 cm) for measurements at 820 nm or in a flat cuvette (thickness 0.8 mm) which was oriented at 45° to the mutually perpendicular measuring and exciting beams for measurements at 480 nm. In order to eliminate dissolved oxygen, the square cuvette was severely degassed under vacuum. Excitation was provided by a ruby laser (Quantel, France; pulse energy ≈15 mJ; wavelength = 694.3 nm; duration ≈6 ns); laser flashes were saturating for PSI photochemistry. The measuring light was provided by a 200 W tungsten-halogen lamp and the appropriate wavelength was selected with interference filters of 10 nm bandwidth placed before and after the cuvette. For measurements at 480 nm, a shutter was placed just before the cuvette and was opened 1.5 ms before the actinic flash was fired, in order to avoid any actinic effect of the measuring light. A biased silicium photodiode was used as detector, and the output signal was filtered and amplified using the 7A22 Tektronix plug-in amplifier (DC-1 MHz) before being recorded and digitized (Tektronix RTD710A coupled to a PC microcomputer). A Marquardt least-squares algorithm was used to fit the kinetics of absorption change to a multiexponential decay.

In the experiments where fast reduction of ferredoxin is occurring, it was also found that some flash-induced scattering changes, with a somewhat longer decay halftime, were superimposed on the related absorption changes. These scattering signals were identified by measuring the apparent flash-induced absorption changes between 750 and 900 nm. In contrast to the two components that were measured at 480 nm (see Results), only the slower of these two components was detected in the near infrared region. As this slower component exhibits a flat spectrum between 750 and 900 nm and therefore cannot be due to the decay of $P700^+$, it was ascribed to a scattering change. For the data shown in Figure 6, the original decay kinetics at 480 nm were fitted to a biexponential decay by fixing the halftime of one of the components to the halftime of the scattering signal that was detected in the near infrared. This last component was then subtracted from the experimental kinetics for an easier comparison of pure absorption changes between different samples.

PSI concentration was estimated assuming an absorption coefficient of 6500 M^{-1} cm^{-1} for $P700^+$ at 820 nm (Mathis and Sétif, 1981). From the transient flash-induced absorption changes at 820 nm, chlorophyll to P700 ratios of 110 ± 10 and 100 ± 10 were estimated respectively for the isolated membranes and for the PSI particles from either the wild type or the *psaE*-deleted strain.

Acknowledgements

We wish particularly to thank D.Dejonghe for constant and skilful technical assistance in molecular biology. We are grateful to Dr F.Chauvat for advice in the field of cyanobacterial genetic engineering. Antibody obtention was carried out and supervised by M.Plaisance and Dr Y.Frobert (SPI, Saclay). Oligonucleotides were made by C.Doira from the laboratory of Dr J.M.Buhler (SBGM, Saclay). Microsequencing was performed using the sequencing facilities provided by Dr A.Menez (DIEPP, Saclay). Part of this work was supported by the Centre National de la Recherche Scientifique (URA 1290).

References

Andersen,B., Scheller,H.V. and Møller,B.L. (1992) *FEBS Lett.*, **311**, 169–173.
Anderson,S.L. and McIntosh,L. (1991) *J. Bacteriol.*, **173**, 2761–2767.
Bengis,C. and Nelson,N. (1977) *J. Biol. Chem.*, **252**, 4564–4569.
Bottin,H. and Lagoutte,B. (1992) *Biochim. Biophys. Acta*, **1101**, 48–56.
Bottin,H. and Sétif,P. (1991) *Biochim. Biophys. Acta*, **1057**, 331–336.
Chauvat,F., De Vries,L., Van der Ende,A. and Van Arkel,G.A. (1986) *Mol. Gen. Genet.*, **204**, 185–191.
Chauvat,F., Rouet,P., Bottin,H. and Boussac,A. (1989) *Mol. Gen. Genet.*, **216**, 51–59.
Chen,E.J. and Seeburg,P.H. (1985) *DNA*, **4**, 165–170.
Chitnis,P.R., Reilly,P.A. and Nelson,N. (1989a) *J. Biol. Chem.*, **264**, 18381–18385.
Chitnis,P.R., Reilly,P.A., Miedel,M.C. and Nelson,N. (1989b) *J. Biol. Chem.*, **264**, 18374–18380.
Drobnica,L., Kristian,P. and Augustin,J. (1977) In Pataï,S. (ed.), *The Chemistry of the Cyanates and their thio Derivatives*. John Wiley and Sons, New York, pp. 1005–1221.
Franzen,L.-G., Frank,G., Zuber,H. and Rochaix,J.-D. (1989) *Plant Mol. Biol.*, **12**, 463–474.
Golbeck,J. (1992) *Annu. Rev. Plant Physiol. Plant Mol. Biol.*, **43**, 293–324.
Golbeck,J.H. and Bryant,D.A. (1991) In Govindjee (ed.), *Current Topics in Bioenergetics*. Academic Press, London, pp. 83–177.
Haselkorn,R. (1991) *Methods Enzymol.*, **204**, 418–430.
Hervas,M., Navarro,J.A. and Tollin,G. (1992) *Photochem. Photobiol.*, **56**, 319–324.
Ke,B. (1973) *Biochim. Biophys. Acta*, **301**, 1–33.
Labarre,J., Chauvat,F. and Thuriaux,P. (1989) *J. Bacteriol.*, **171**, 3449–3457.
Laemmli,U.K. (1970) *Nature*, **227**, 680–685.
Lagoutte,B. and Vallon,O. (1992) *Eur. J. Biochem.*, **205**, 1175–1185.
Li,N., Zhao,J., Warren,P.V., Warden,J.T., Bryant,D.A. and Golbeck,J.H. (1991a) *Biochemistry*, **30**, 7863–7872.
Li,N., Warren,P.V., Golbeck,J.H., Frank,G., Zuber,H. and Bryant,D.A. (1991b) *Biochim. Biophys. Acta*, **1059**, 215–225.
Mannan,R.M., Whitmarsh,J., Nyman,P. and Pakrasi,H.B. (1991) *Proc. Natl. Acad. Sci. USA*, **88**, 10168–10172.
Marck,C. (1988) *Nucleic Acids Res.*, **16**, 1829–1836.
Mathis,P. and Sétif,P. (1981) *Isr. J. Chem.*, **21**, 316–320.
Mitchinson,C., Wilderspin,A.F., Trinnaman,B.J. and Green,N.M. (1982) *FEBS Lett.*, **146**, 87–92.
Münch,S., Ljungberg,U., Steppuhn,J., Schneiderbauer,A., Nechushtai,R., Beyreuther,K. and Herrmann,R.G. (1988) *Curr. Genet.*, **14**, 511–518.

Oh-oka,H., Takahashi,Y. and Matsubara,H. (1989) *Plant Cell Physiol.*, **30**, 869–875.
Okkels,J.S., Jepsen,L.B., Hønberg,L.S., Lehmbeck,J., Scheller,H.V., Brandt,P., Høyer-Hansen,G., Stummann,B., Henningsen,K.W., von Wettstein,D. and Møller,B.L. (1988) *FEBS Lett.*, **237**, 108–112.
Ortiz,W., Lam,E., Chollar,S., Munt,D. and Malkin,R. (1985) *Plant Physiol.*, **77**, 389–397.
Pakrasi,H.B., Williams,J.G.K. and Arntzen,C.J. (1988) *EMBO J.*, **7**, 325–332.
Pick,U. and Karlish,S.J.D. (1980) *Biochim. Biophys. Acta*, **626**, 255–261.
Porter,R.D. (1988) *Methods Enzymol.*, **167**, 703–712.
Rippka,R., Deruelles,J., Waterbury,J.B., Herdmann,M. and Stanier,R.Y. (1979) *J. Gen. Microbiol.*, **111**, 1–61.
Rousseau,F. and Lagoutte,B. (1990) *FEBS Lett.*, **260**, 241–244.
Sanger,F., Nicklen,S. and Coulson,A.R. (1977) *Proc. Natl. Acad. Sci. USA*, **74**, 5463–5467.
Schägger,H., and Von Jagow,G. (1987) *Anal. Biochem.*, **166**, 368–379.
Sétif,P. and Bottin,H. (1989) *Biochemistry*, **28**, 2689–2697.
Sétif,P., Ikegami,I. and Biggins,J. (1987) *Biochim. Biophys. Acta*, **894**, 146–156.
Shestakov,S.V. and Khyen,N.T. (1970) *Mol. Gen. Genet.*, **107**, 372–375.
Smart,L.B., Anderson,S.L. and McIntosh,L. (1991) *EMBO J.*, **10**, 3289–3296.
Tandeau de Marsac,N., Borrias,W.E., Kuhlemeier,C.J., Castets,A.M., van Arkel,G.A. and van den Hondel,C.A.M.J.J. (1982) *Gene*, **20**, 111–119.
Tietze,F., Mortimore,G.E. and Lomax,N.R. (1962) *Biochim. Biophys. Acta*, **59**, 336–346.
Toelge,M., Ziegler,K., Maldener,I. and Lockau,W. (1991) *Biochim. Biophys. Acta*, **1060**, 233–236.
Vermaas,W.F.J., Williams,J.G.K., Rutherford,A.W., Mathis,P. and Arntzen,C.J. (1986) *Proc. Natl. Acad. Sci. USA*, **83**, 9474–9477.
Williams,J.G.K. (1988) *Methods Enzymol.*, **167**, 766–778.
Zanetti,G. and Merati,G. (1987) *Eur. J. Biochem.*, **169**, 143–146.
Zilber,A.L. and Malkin,R. (1988) *Plant Physiol.*, **88**, 810–814.
Zilber,A.L. and Malkin,R. (1992) *Plant Physiol.*, **99**, 901–911.

Received on November 12, 1992; revised on February 10, 1993